[redacted]



NACA RM SL54K18a

R.A. A73L87 R.M.1



NACA

# RESEARCH MEMORANDUM

for the

U. S. Air Force

## EFFECTS OF FUSELAGE MODIFICATIONS ON THE DRAG CHARACTERISTICS OF A 1/20-SCALE MODEL OF THE CONVAIR F-102 AIRPLANE AT TRANSONIC SPEEDS

By Thomas C. Kelly and Robert S. Osborne

Langley Aeronautical Laboratory
Langley Field, Va.



CLASSIFIED DOCUMENT

This material contains information affecting the National Defense of the United States within the meaning of the espionage laws, Title 18, U.S.C., Secs. 793 and 794, the transmission or revelation of which in any manner to an unauthorized person is prohibited by law.

NATIONAL ADVISORY COMMITTEE
FOR AERONAUTICS

WASHINGTON

[redacted]

NACA RM SL54K18a

NATIONAL ADVISORY COMMITTEE FOR AERONAUTICS

RESEARCH MEMORANDUM

for the

U. S. Air Force

# EFFECTS OF FUSELAGE MODIFICATIONS ON THE DRAG CHARACTERISTICS OF A 1/20-SCALE MODEL OF THE CONVAIR F-102 AIRPLANE AT TRANSONIC SPEEDS

By Thomas C. Kelly and Robert S. Osborne

## SUMMARY

An investigation has been conducted in the Langley 8-foot transonic tunnel to determine the effects of several fuselage modifications on the transonic drag-rise characteristics of a 1/20-scale model of the Convair F-102 airplane. Tests covered an angle-of-attack range from $0^{\circ}$ to about $10^{\circ}$ and a Mach number range from 0.60 to 1.14.

Results indicated that the transonic drag rise for the basic F-102 airplane could be substantially reduced by extending the fuselage afterbody approximately 8 percent of the fuselage length. Tests of other bodies indicated that a shorter (4-percent) afterbody extension may have a similar effect on the drag rise. Further improvement of the axial cross-sectional-area distribution of the 8-percent extended configuration through the addition of fuselage volume resulted in additional reductions in the drag rise at a Mach number of 1.0 and caused no or only slight drag penalties at the higher Mach numbers.

The results of the present tests generally substantiate the area-rule concept with respect to the prediction of the transonic drag rise through the use of an equivalent-area body of revolution for a practical delta-wing airplane configuration.

## INTRODUCTION

At the request of the U. S. Air Force, an investigation of a 1/20-scale model of the Convair F-102 interceptor airplane has been conducted in the Langley 8-foot transonic tunnel to determine its stability, control, and performance characteristics. The results of the initial tests (ref. 1) indicated that the original configuration had an undesirably high zero-lift transonic drag rise. In an effort to reduce the drag rise several fuselage modifications were made to the configuration. These modifications were designed to improve the axial distribution of cross-sectional area of the configuration and to be applicable to the original airplane without requiring extensive redesign. The results of force tests of the modified configurations at Mach numbers from 0.60 to 1.14 and angles of attack from $0^\circ$ to about $10^\circ$ are presented herein. In addition, in order to check the applicability of the equivalent-body concept (see ref. 2) to practical delta-wing airplane configurations, a body of revolution with the same area distribution as the basic configuration was tested.

The results of tests of some of these configurations at Mach numbers of 1.41 and 2.01 are presented in reference 3.

## SYMBOLS

$A_E$ duct exit area, sq ft

$C_D$ external-drag coefficient, $C_{D_m}$ with ducts closed and $C_{D_m} - C_{D_I}$ with ducts open

$\Delta C_D$ incremental drag coefficient, drag coefficient at any Mach number minus drag coefficient at $M = 0.60$

$C_{D_I}$ internal-drag coefficient, $D_I/qS$

$C_{D_m}$ measured drag coefficient, adjusted to free-stream static pressure at model base, $D_m/qS$

$C_{D_o}$ drag coefficient at zero lift

$\Delta C_{D_o}$ incremental zero-lift drag coefficient, zero-lift drag coefficient at any Mach number minus zero-lift drag coefficient at $M = 0.60$

$C_L$ lift coefficient, $L/qS$

$\frac{\partial C_L}{\partial \alpha}$ lift-curve slope per degree, averaged from $\alpha = 0^\circ$ over linear portion of curve

$C_m$ pitching-moment coefficient, $\frac{M_{cg}}{qS\bar{c}}$

$\frac{\partial C_m}{\partial C_L}$ static-longitudinal-stability parameter, averaged from $C_L = 0$ over linear portion of curve

$\bar{c}$ wing mean aerodynamic chord, in.

$D_m$ measured drag, adjusted to free-stream static pressure at model base, lb

$D_I$ internal drag, $m\left(V_O - V_E\right) - A_E\left(p_E - p_O\right)$, lb

L lift, lb

M free-stream Mach number

$M_{cg}$ pitching moment about center-of-gravity location at $0.275\bar{c}$ and $0.036\bar{c}$ above wing-chord plane, in-lb

m mass flow through inlets, slugs/sec

$m_O$ mass flow in free-stream tube of area equal to projected inlet area at $\alpha = 0^\circ$, slugs/sec

$m/m_O$ inlet mass-flow ratio

$P_b$ base pressure coefficient, $\frac{p_b - p_O}{q}$

$p_b$ static pressure at model base, lb/sq ft

$p_E$ static pressure at duct exit, lb/sq ft

$p_O$ free-stream static pressure, lb/sq ft

q free-stream dynamic pressure, lb/sq ft

S total wing area including that part within fuselage, sq ft

$V_E$ velocity in duct exit, ft/sec

$V_o$ free-stream velocity, ft/sec

$\alpha$ angle of attack of wing-chord line, deg

## APPARATUS AND METHODS

### Tunnel

The Langley 8-foot transonic tunnel is a single-return, dodecagonal, slotted-throat wind tunnel designed to obtain aerodynamic data through the speed of sound while minimizing the usual effects of blockage (see ref. 4). The tunnel operates at a stagnation pressure which is close to atmospheric. A more complete description of this facility may be found in reference 5.

### Model Support System

The models were mounted on an internal electrical strain-gage balance and were sting supported in the tunnel. Various sting angular couplings were used to keep the models near the tunnel center line at all angles of attack.

### Models

The 1/20-scale model of the F-102 was provided by the contractor. Dimensions and details of the basic configuration are presented in figure 1 and table I.

The delta wing had 60° sweptback leading edges, 5° sweptforward trailing edges, and modified NACA 0004-65 airfoil sections parallel to the airstream. Chordwise fences extending from the wing leading edges to the elevons were installed at the 66-percent-semispan stations. Fence details and wing airfoil ordinates are available in reference 1. The vertical tail had the same plan form and airfoil sections as the basic wing semispan and included a flat-plate antenna located above the rudder.

The fuselage of the basic configuration had a 5° drooped nose with probe, a V-type canopy with a leading-edge slope of 30°, and twin ram inlets with external boundary-layer bleedoff and internal ducting to the model base. For the ducts-closed tests, faired plugs were installed in the inlets. It should be noted that the basic configuration of the present investigation differed from that of reference 1 in that the nose and canopy were revised and the chordwise fences and elevon horns were

located at slightly different semispan stations. Other slight geometric variations between the two models (see tables I of ref. 1 and the present paper) resulted from inadvertent differences in model construction.

The basic model of the F-102 tested contained several compromises with respect to a true 1/20-scale model. The following design changes were made to the full-scale prototype airplane subsequent to construction of the model tested and therefore were not incorporated in it: The diameter of the fuselage was increased 4 inches (0.2 inch, 1/20-scale) because of an increase in armament size; in order to keep the exposed wing area the same, the wings were moved outboard 2 inches (0.1 inch, 1/20-scale), so that an increase of 1.77 percent in total wing area resulted; and the inlets were moved forward about 20 inches, (1 inch, 1/20-scale). In addition, the base diameter of the model tested was enlarged 0.3 inch over that for a true 1/20-scale model in order to insure that the minimum-area section for the duct system would occur near the inlets with the sting in place. The average boattail angle of the model tested was approximately $2^{\circ}$ less than that of the full-scale airplane.

The first fuselage modification, called the 2.3-inch-extended configuration, was designed to increase the basic-afterbody fineness ratio and improve its area distribution. The modification consisted of extending the basic afterbody 2.3 inches (46 inches, full-scale) while holding the base area constant, as shown in figures 2 and 3(a). A second modification, designated the smooth-added-volume configuration, was designed to give smooth axial distributions of total cross-sectional area for the upper and lower portions of the 2.3-inch-extended fuselage configuration (the dividing plane being taken as the wing-chord plane) in the region between the canopy and the maximum-area location. Plastic fairings were added to the 2.3-inch-extended fuselage above and below the wing-chord plane in the region between the canopy and the vertical fin as shown in figures 2, 3(a), and 3(b). The maximum frontal area of the fuselage was increased about 21 percent. The third fuselage modification was similar to the second except that the rearward portion of the plastic fairing below the wing-chord plane was shortened to produce an indentation in the lower-surface area distribution just back of the leading edges of the inboard sections of the wing (see figs. 2, 3(a), and 3(b)). For this configuration, designated the indented-added-volume configuration, the basic maximum fuselage frontal area was increased approximately 16 percent.

A body of revolution having the same axial distribution of cross-sectional area as the complete basic configuration with the ducts closed and the probe removed was also tested. This is referred to herein as the equivalent body for the basic configuration.

Two bodies of revolution were tested in combination with the 1/20-scale basic wing that had chordwise fences. The first body had an axial distribution of cross-sectional area identical to that of the

1/20-scale basic fuselage with the ducts closed and the tail, canopy, and probe removed (fig. 3(c)). This configuration is referred to herein as the wing with body of revolution for basic fuselage less canopy and tail. The second configuration, designated the wing with body of revolution for basic fuselage less canopy and tail with 1.2-inch extension, was designed to increase the afterbody fineness ratio and to improve its area distribution (fig. 3(c)). This modification consisted of holding the base area constant and extending the afterbody 1.2 inches (24 inches, full-scale) as shown in figure 3(c).

## Measurements and Accuracy

Lift, drag, and pitching moment were measured by means of the internal strain-gage balance. Coefficients are based on the total wing area of 1.625 square feet. Pitching-moment coefficients, based on a mean aerodynamic chord of 13.755 inches, are referred to a center-of-gravity location which was at 27.5 percent of the mean aerodynamic chord and 3.6 percent of the mean aerodynamic chord above the wing-chord plane. Based upon balance accuracies and repeatability of data, the coefficients are estimated to be accurate within the following limits for lift coefficients to at least 0.4:

| | |
|---|---|
| $C_L$ | $\pm 0.005$ |
| $C_{D_m}$ | $\pm 0.001$ |
| $C_m$ | $\pm 0.001$ |

Mass flow through the ducts and internal drag were determined from pressure measurements made with a survey rake located at the model base (see fig. 1(b)). As shown, a total of five static- and fourteen total-pressure orifices were arranged in the duct-exit annulus in order to cover five equal portions of the exit area. Internal-drag coefficients are estimated to be accurate within $\pm 0.001$. For all configurations except those with the ducts open, base pressure measurements were made by using an orifice located on the sting support just forward of the plane of the model base. Base pressure coefficients are estimated to be accurate to within $\pm 0.005$.

Model angle of attack, determined by means of a fixed-pendulum strain-gage unit located in the sting support and a calibration of sting and balance deflection under various loadings, is estimated to be accurate within $\pm 0.15^\circ$.

Local deviations from the average free-stream Mach number did not exceed 0.003 at subsonic speeds and did not become greater than about 0.01 as the Mach number was increased to 1.14 (ref. 5).

## Tests

All models were tested at Mach numbers from 0.60 to 1.14. The basic, 2.3-inch-extended, and added-volume configurations with the ducts open, and the basic configuration with the ducts closed were tested at angles of attack from $0^\circ$ to about $10^\circ$. The basic configuration with the canopy, probe, and tail removed, the equivalent-body configuration, and the wing in combination with the bodies of revolution were tested with the ducts closed through the Mach number range at $0^\circ$ angle of attack only.

Mass-flow and internal-force data were obtained for the basic configuration only.

Reynolds numbers for the present tests were on the order of $4.4 \times 10^6$, based on the wing mean aerodynamic chord (fig. 4).

## Corrections

Subsonic boundary-interference effects in the slotted test section are considered negligible, and, therefore, no corrections for these effects have been applied. In an effort to reduce the effects of boundary-reflected expansion and compression waves, the model was tested in a position vertically offset from the tunnel center line by about 5 inches at an angle of attack of $0^\circ$ (this procedure reduces the shock-focusing effects). In addition, the analysis plots have been faired to minimize the effects of boundary-reflected disturbances. (See ref. 6.)

Although no adjustments for the effects of sting interference have been applied, the effects have been reduced for the ducts-closed configurations by adjusting all the data to a condition representing free-stream static pressure at the model base, and for the ducts-open configurations by presenting only external drag in the analysis plots.

Internal-drag data obtained for the basic configuration have been used to adjust measured drag values for the 2.3-inch-extended and added-volume configurations for which no internal-flow measurements were made. The assumption is made that the effects of afterbody extension and volume addition on the internal-drag characteristics are small. Base pressure coefficients for the various configurations are presented in figure 5. Mass-flow and internal-drag characteristics for the basic configuration are shown in figure 6.

Because of the differences in body size and profile noted earlier, it would be expected that the transonic zero-lift drag rise for an exact 1/20-scale model of the prototype airplane would be somewhat higher than that for the model tested. By using the method shown in the correlation of reference 7, the difference in peak pressure-drag coefficient for the

two configurations has been calculated. The zero-lift peak pressure-drag coefficient for an exact 1/20-scale model was estimated to be about 0.0025 or 15 percent higher than the value of 0.017 obtained at a Mach number of 1.08 for the model tested, and, although this adjustment has not been applied to the data presented in the present paper, it should be taken into consideration if a correlation with full-scale flight results is attempted.

## RESULTS AND DISCUSSION

Basic force and moment data for the various configurations are shown in figures 7 to 10. Analysis figures, obtained from the basic plots, are presented as figures 11 to 15. In order to facilitate presentation of the data, staggered scales have been used in some figures and care should be taken in selecting the zero axis for each curve.

### Modifications to the Basic Fuselage

General.- By using the transonic area-rule concept as a basis for reducing the drag at Mach numbers near 1.0, modifications have been made to the basic fuselage in order to improve the axial distribution of cross-sectional area for the complete configuration. Afterbody extensions of 2.3 and 1.2 inches (46 and 24 inches, full-scale, respectively) have been designed to obtain a more gradual contraction of area at the rearward end of the model for the purpose of reducing the induced velocities in the region of the wing trailing edge. Earlier verifications of the area rule (ref. 8, for example) have indicated that transonic drag may be reduced considerably by such changes. Similarly, the addition of fuselage volume to the 2.3-inch-extended configuration was designed to fill in the depression in the area-distribution curve between peaks caused by the air-inlet—canopy and wing—vertical-tail combinations (fig. 3(a)) in order to reduce somewhat the induced velocities in the general flow field associated with these peaks. This modification was of an exploratory nature and was made to indicate the possibility of decreasing transonic drag by adding volume to the configuration. The added-volume configuration with a fairly abrupt contraction of volume on the lower surface just rearward of the inboard wing leading edge was based on the results presented in reference 9, which indicated that drag-due-to-lift characteristics would be improved by a modification of this type.

Drag at zero lift.- Drag polars for the basic and modified fuselage configurations are shown in figures 7 to 9. Zero-lift and incremental zero-lift drag coefficients (based on the drag at a Mach number of 0.60) are plotted against Mach number in figure 11. Comparison of the incremental zero-lift drag coefficient (taken at a Mach number of 1.07) for

the basic configuration of reference 1 with that of the present tests indicates that the drag rise was reduced by about 0.002 in drag coefficient as a result of the change to a sharper nose and the V-type canopy.

The zero-lift drag data of the present tests show that, as the area distribution was improved by the 2.3-inch afterbody extension and addition of fuselage volume, there was a corresponding reduction in the drag level at subsonic speeds. Reasons for the changes in the subsonic level are not known. They may be associated with the boundary-layer transition occurring at different positions on the various configurations because changes in model surface condition (see ref. 10) may have been critical in the Reynolds number range of these tests. It may also be possible that the fuselage modifications caused changes in the interference effects existing between the different model components. Because these changes in subsonic drag level may not occur at full-scale flight Reynolds numbers, the incremental drag coefficients are probably of most interest.

Figure 11 shows that at the design Mach number of 1.0 the incremental zero-lift drag coefficient for the basic configuration (based on the drag at a Mach number of 0.60) was reduced from about 0.014 to about 0.010 or 29 percent as a result of the 2.3-inch afterbody extension. Addition of the indented and smooth volume to the 2.3-inch-extended configuration resulted in values of the incremental zero-lift drag coefficients of about 0.009 and 0.008, respectively, or overall drag-rise reductions of 36 and 43 percent.

Comparison of the incremental zero-lift drag coefficients at a Mach number of about 1.07 indicates that the initial reduction of about 12 percent in the drag rise obtained by the afterbody extension was changed only slightly by the addition of fuselage volume. The results shown are particularly interesting in that it was possible to increase the fuselage volume and frontal area and still obtain drag reduction at a Mach number of 1.0 and only a slight drag penalty for the indented-added-volume configuration or no drag penalty for the smooth-added-volume configuration up to the highest test Mach number.

Because of possible tailpipe-length and ground-clearance problems with the 2.3-inch (46 inches, full-scale) extension, an effort was made to determine whether a shorter afterbody extension would be effective in reducing the transonic drag. The results, shown in figure 12, indicate that a 1.2-inch (24 inches, full-scale) extension to a configuration composed of the basic wing with a body of revolution representing the basic fuselage less canopy and tail reduced the transonic drag rise taken between Mach numbers of 0.60 and 1.07 by an amount close to that obtained with the 2.3-inch-extended configuration. Though the two extended configurations are not directly comparable, incremental drag changes resulting from the afterbody extension do provide an indication that the shorter extension may be satisfactory.

[redacted]

Drag at lifting conditions.- Drag coefficients and incremental drag coefficients for the basic and modified fuselage configurations are shown in figure 13 at several lift coefficients. The subsonic drag differences shown in figure 13(a) may not occur or be of the same magnitude at full-scale flight Reynolds number (see discussion of subsonic drag levels at zero lift). Hence, most of the discussion pertains to the incremental drag coefficients of figure 13(b). As for the zero-lift case, most noticeable reductions in the transonic incremental drag coefficients occur as a result of the 2.3-inch afterbody extension. At a Mach number of 1.0 and a lift coefficient of 0.2, the reduction in incremental drag coefficient amounted to about 0.006. Addition of fuselage volume to the extended configuration resulted in an overall reduction of 0.008. Increases in lift coefficient above 0.2 and Mach numbers above 1.0 had relatively little effect on the drag reduction due to fuselage extension but generally decreased the reductions due to adding fuselage volume.

Comparison of the drag data for the smooth- and indented-added-volume configurations (figs. 9 and 13) indicates that no advantage in drag due to lift was gained as a result of the lower-surface volume indentation.

Lift and pitching-moment characteristics.- The variation of lift coefficient with angle of attack for the basic and modified fuselage configurations, shown in figures 7 to 9, indicates some minor effects due to opening the ducts for the basic configuration and modifying the fuselage by afterbody extension and volume addition. Lift-curve slopes (fig. 14) show slightly favorable effects resulting from fuselage modifications at Mach numbers above 0.80 for the 2.3-inch-extended configuration and 0.98 for the added-volume configurations.

Pitching-moment characteristics for the basic and modified fuselage configurations, shown in figures 7, 8, 9 and 14, indicate only minor effects due to fuselage modification.

## Area-Rule Body Configurations

General.- Initial comparisons of various wing-body combinations with their equivalent bodies of revolution (ref. 2) indicated close drag-rise agreement for a delta-wing research configuration having a high-fineness-ratio body and smooth body contours. Tests discussed in this section were made to study the transonic-drag-rise agreement between the basic configuration and its equivalent body and between the basic configuration less canopy and tail and the wing with a body of revolution representing the basic fuselage less canopy and tail, all with the ducts closed. These configurations, having relatively low fineness ratio bodies, include protuberances such as the inlets which cause rather abrupt changes in the axial cross-sectional-area distributions.

Drag characteristics.- The results of the area-rule body tests are shown in figure 15. Values of the incremental zero-lift drag coefficients (taken between Mach numbers of 0.60 and 1.07) for the basic configuration and its equivalent-area body of revolution were about 0.018 and 0.019, respectively; these values indicate excellent agreement for the two configurations. The difference in drag level shown throughout the Mach number range is associated with the lack of wing skin friction for the equivalent body. These data, therefore, substantiate the area-rule concept with respect to the prediction of the transonic drag rise through the use of an equivalent-area body of revolution for a practical delta-wing airplane configuration.

The variation of drag coefficient with Mach number for the basic configuration less canopy and tail and the wing with a body of revolution representing the basic fuselage less canopy and tail shows excellent agreement in both the subsonic drag level and the transonic drag rise for the two configurations.

It is of interest to note in figure 15 that removal of the canopy and tail from the basic configuration resulted in a reduction in the incremental zero-lift drag coefficient of about 0.004, or 23 percent (taken at a Mach number of 1.07), due mainly to the improvement in area distribution for the configuration (see fig. 3(a)) and the attendant reduction of induced velocities in these critical area regions. Analysis using the method of reference 7 indicated that the contributions of the tail and canopy to the noted drag reduction are about equal.

It should be pointed out that, although changes in area distribution had the major effect, some improvement in the transonic drag-rise characteristics would be associated with decreases in frontal area. Presented in table II are values of maximum frontal area, equivalent-body fineness ratio, and incremental zero-lift drag-rise coefficients (taken between Mach numbers of 0.60 and about 1.07) for the various configurations tested in order to indicate the magnitude of the changes which occurred and to provide a general comparison for all configurations tested.

## CONCLUSIONS

An investigation of fuselage modifications to a 1/20-scale model of the Convair F-102 airplane in the Langley 8-foot transonic tunnel has led to the following conclusions:

1. The transonic drag rise between Mach numbers of 0.60 and about 1.07 for the basic configuration was reduced about 12 percent by the addition of a 2.3-inch afterbody extension to the basic fuselage. Tests of the basic wing in combination with two bodies of revolution indicated

that a 1.2-inch afterbody extension may have a similar effect on the transonic drag rise.

2. Further improvement of the axial cross-sectional-area distribution for the 2.3-inch-extended configuration by the addition of fuselage volume resulted in additional reductions in the drag rise at a Mach number of 1.0 and caused no or only slight drag penalties at the higher Mach numbers.

3. Results of the present tests substantiate the area-rule concept with respect to the prediction of the transonic drag rise through the use of an equivalent-area body of revolution for a practical delta-wing airplane configuration.

Langley Aeronautical Laboratory,
National Advisory Committee for Aeronautics,
Langley Field, Va., November 2, 1954.

Thomas C. Kelly
Aeronautical Research Scientist

Robert S. Osborne
Aeronautical Research Scientist

Approved: Eugene C. Draley
Eugene C. Draley
Chief of Full-Scale Research Division

mld

## REFERENCES

1. Osborne, Robert S., and Wornom, Dewey E.: Aerodynamic Characteristics Including Effects of Wing Fixes of a 1/20-Scale Model of the Convair F-102 Airplane at Transonic Speeds. NACA RM SL54C23, U. S. Air Force, 1954.

2. Whitcomb, Richard T.: A Study of the Zero-Lift Drag-Rise Characteristics of Wing-Body Combinations Near the Speed of Sound. NACA RM L52H08, 1952.

3. Hilton, John H., Jr., and Palazzo, Edward B.: Wind-Tunnel Investigation of a Modified 1/20-Scale Model of the Convair MX-1554 Airplane at Mach Numbers of 1.41 and 2.01. NACA RM SL53G30, U. S. Air Force, 1953.

4. Wright, Ray H., and Ward, Vernon G.: NACA Transonic Wind-Tunnel Test Sections. NACA RM L8J06, 1948.

5. Ritchie, Virgil S., and Pearson, Albin O.: Calibration of the Slotted Test Section of the Langley 8-Foot Transonic Tunnel and Preliminary Experimental Investigation of Boundary Reflected Disturbances. NACA RM L51K14, 1952.

6. Osborne, Robert S., and Mugler, John P., Jr: Aerodynamic Characteristics of a 45° Sweptback Wing-Fuselage Combination and the Fuselage Alone Obtained in the Langley 8-Foot Transonic Tunnel. NACA RM L52E14, 1952.

7. Nelson, Robert L., and Stoney, William E., Jr: Pressure Drag of Bodies at Mach Numbers up to 2.0. NACA RM L53I22c, 1953.

8. Kelly, Thomas C.: Transonic Wind-Tunnel Investigation of the Aerodynamic Characteristics of a 60° Triangular Wing in Combination With a Systematic Series of Three Bodies. NACA RM L52L22a, 1953.

9. Loving, Donald L.: A Transonic Wind-Tunnel Investigation of the Effect of Modifications to an Indented Body in Combination With a 45° Sweptback Wing. NACA RM L53F02, 1953.

10. Bingham, Gene J., and Braslow, Albert L.: Subsonic Investigation of Effects of Body Indentation on Zero-Lift Drag Characteristics of a 45° Sweptback Wing-Body Combination With Natural and Fixed Boundary-Layer Transition Through a Range of Reynolds Number From $1 \times 10^6$ to $8 \times 10^6$. NACA RM L54B18a, 1954.

[redacted]

TABLE I.- DIMENSIONS OF THE 1/20-SCALE MODEL OF THE F-102 AIRPLANE

| | |
|---|---|
| Wing: | |
| Airfoil section | NACA 0004-65 (Mod.) |
| Total area, sq ft | 1.625 |
| Span, in. | 22.68 |
| Mean aerodynamic chord, in. | 13.755 |
| Aspect ratio | 2.2 |
| Taper ratio | 0 |
| Incidence, deg | 0 |
| Dihedral, deg | 0 |
| Longitudinal location of center of gravity, percent $\bar{c}$ | 27.5 |
| Vertical location of center of gravity above wing-chord plane, percent $\bar{c}$ | 3.6 |
| Leading-edge radius, percent local chord (measured streamwise) | 0.18 |
| Fuselages: | |
| Length, basic, in. | 30.25 |
| Length, 2.3-inch-extended and added-volume configurations, in. | 32.55 |
| Base area, all, sq ft | 0.0349 |
| Projected inlet area at $\alpha = 0^{\circ}$, sq ft | 0.0111 |
| Duct exit area (excluding sting), sq ft | 0.0196 |
| Vertical tail: | |
| Airfoil section | NACA 0004-65 (Mod.) |
| Exposed area, sq ft | 0.1704 |
| Aspect ratio | 1.1 |
| Taper ratio | 0 |

TABLE II.- CHARACTERISTICS OF THE MODELS TESTED

| Configuration | Duct condition | Fuselage length, in. | Maximum cross-sectional area, sq in. | Equivalent-body fineness ratio | Maximum fuselage frontal area, less canopy, sq in. | Fuselage fineness ratio, less canopy | Peak pressure-drag coefficient (based on $C_D$ at M = 0.60) |
|---|---|---|---|---|---|---|---|
| Basic | Open | 30.25 | 16.80 | 6.5 | 10.80 | 8.2 | 0.017 |
| 2.3-inch-extended | Open | 32.55 | 16.80 | 7.0 | 10.80 | 8.8 | .015 |
| Smooth-added-volume | Open | 32.55 | 16.80 | 7.0 | 13.16 | 8.0 | .014 |
| Indented-added-volume | Open | 32.55 | 16.80 | 7.0 | 12.66 | 8.1 | .015 |
| Basic | Closed | 30.25 | 16.80 | 6.5 | 10.80 | 8.2 | .018 |
| Equivalent body for basic | Closed | 30.25 | 16.80 | 6.5 | ----- | --- | .019 |
| Basic less canopy and tail | Closed | 30.25 | 16.42 | 6.6 | 10.80 | 8.2 | .014 |
| Wing with equivalent body for basic fuselage less canopy and tail | Closed | 30.25 | 16.42 | 6.6 | 10.80 | 8.2 | .015 |
| Wing with equivalent body for basic fuselage less canopy and tail with 1.2-inch extension | Closed | 31.45 | 16.42 | 6.9 | 10.80 | 8.5 | .012 |

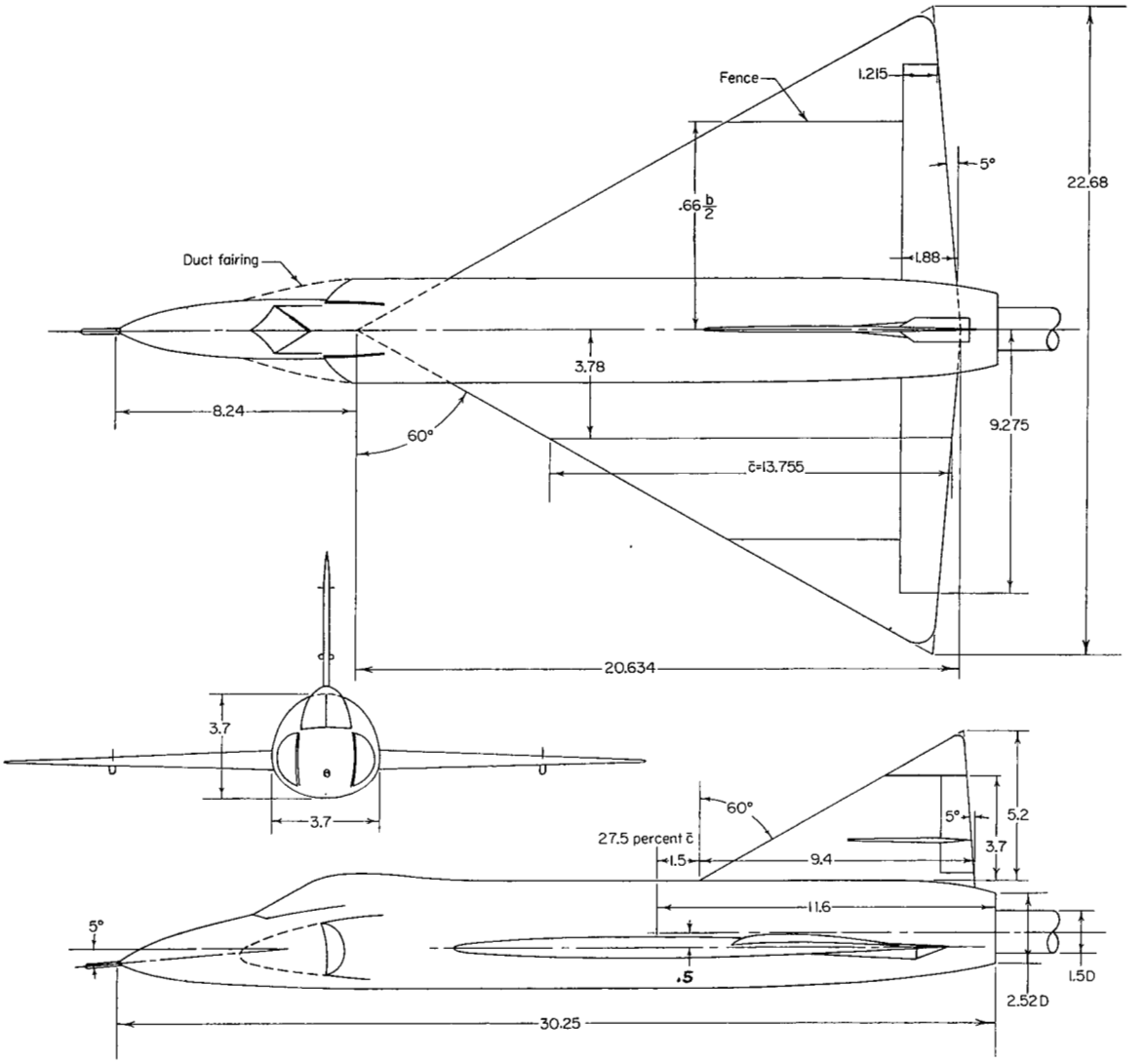


(a) Basic configuration. All dimensions in inches unless otherwise noted.

Figure 1.- Model details.

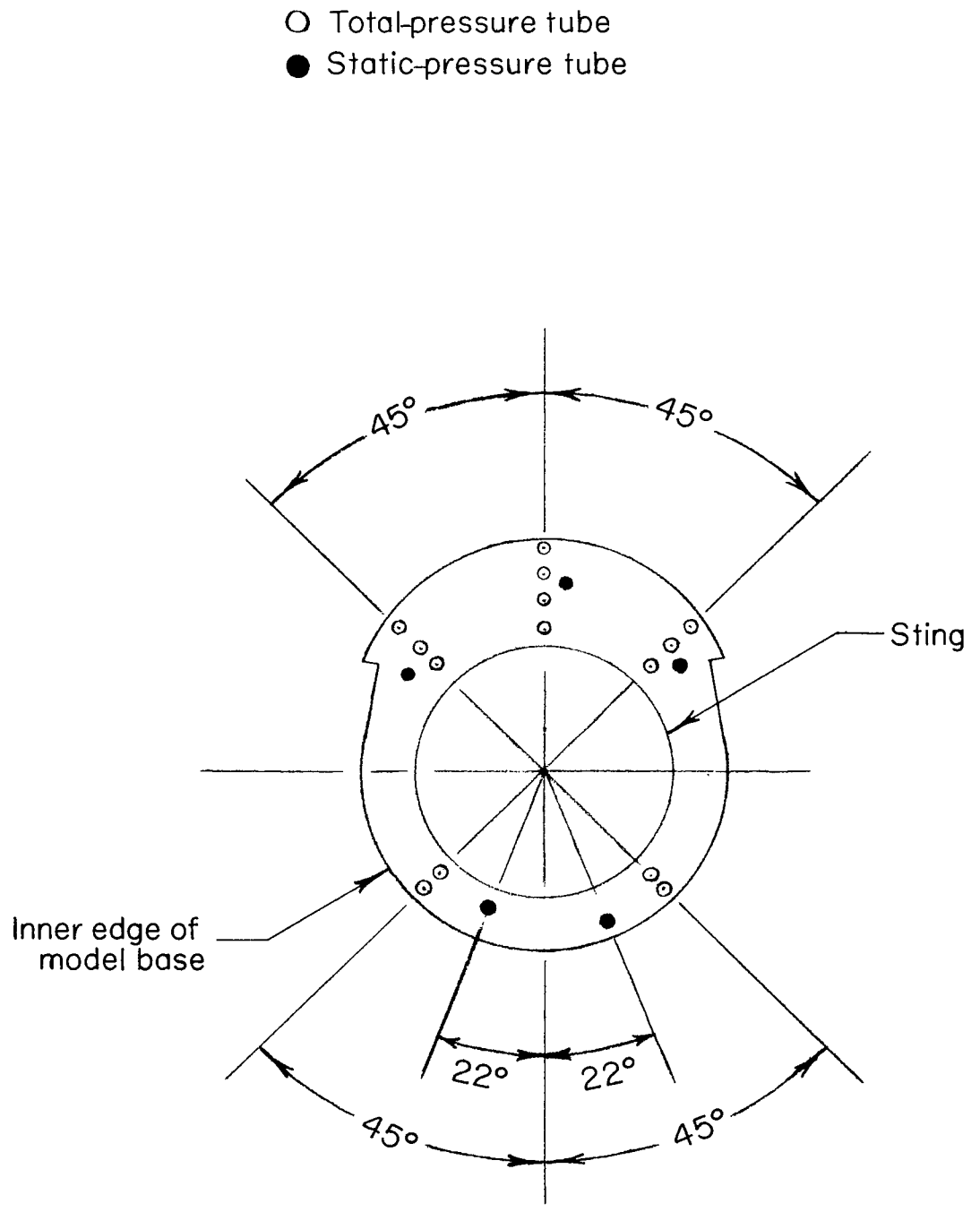


(b) Pressure-tube locations for the duct-exit survey rake.

Figure 1.- Concluded.

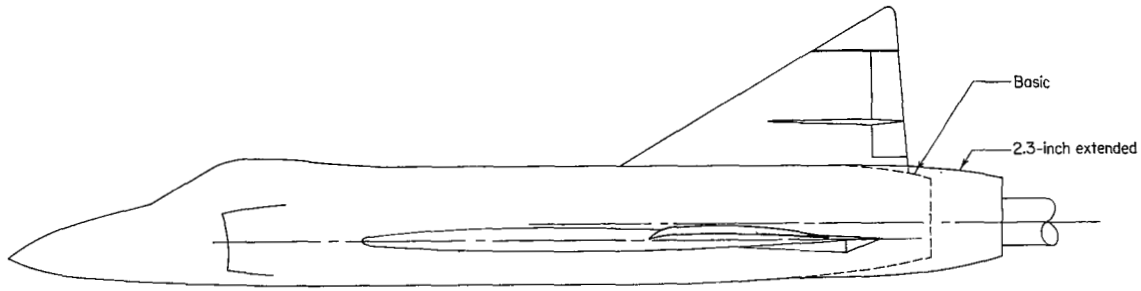


Note: Smooth- and indented-added-volume configurations are modifications of the 2.3-inch-extended configuration shown above.

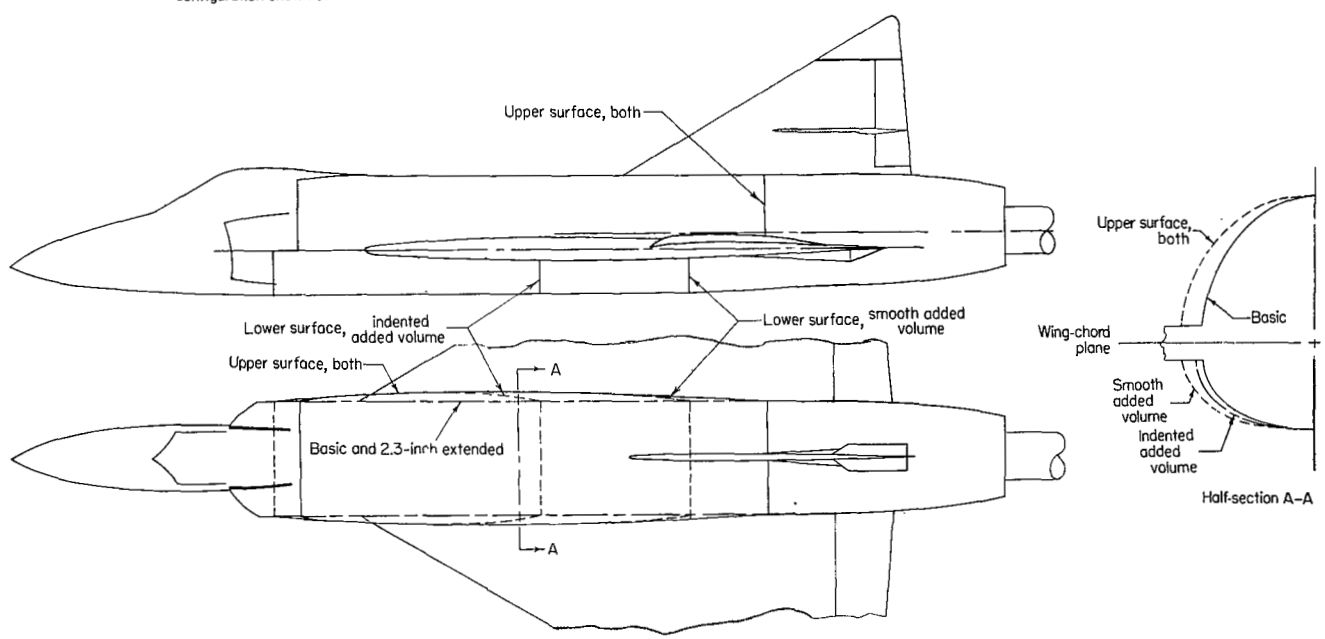


Figure 2.- Details of the modified fuselage configurations.

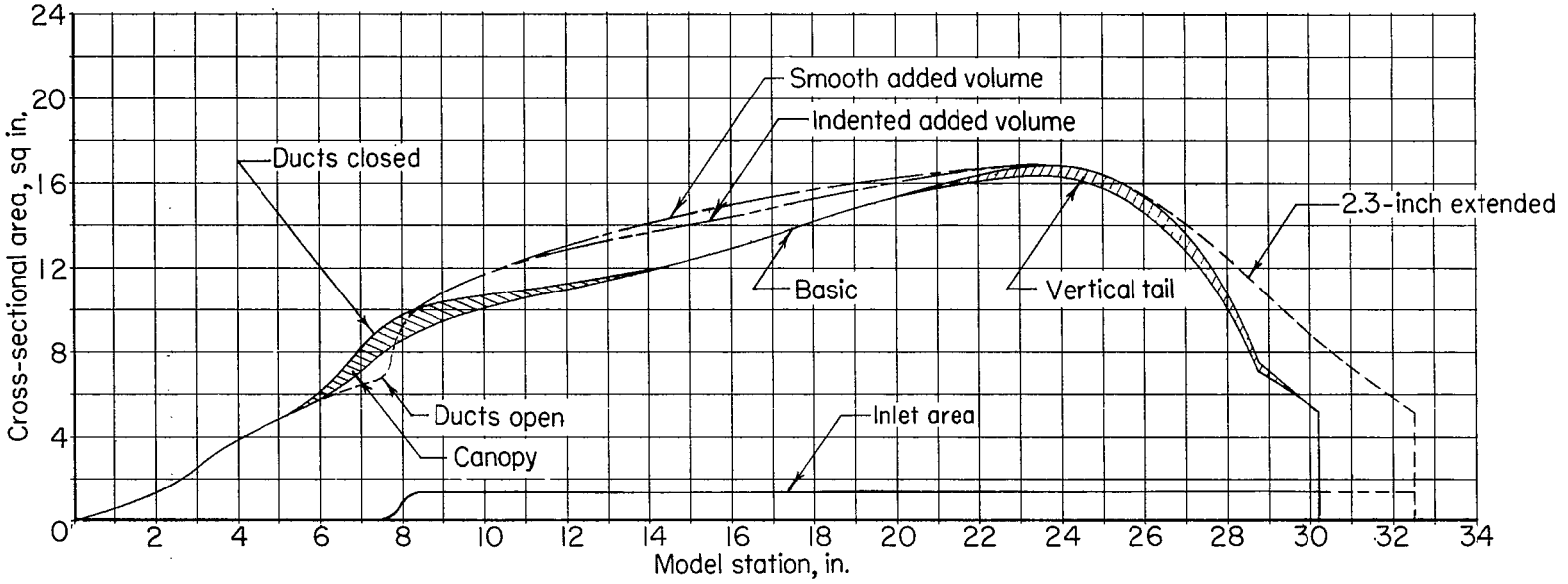


(a) Basic, 2.3-inch-extended, and added-volume configurations. Inlet area not removed.

Figure 3.- Axial distributions of cross-sectional area for the various configurations.

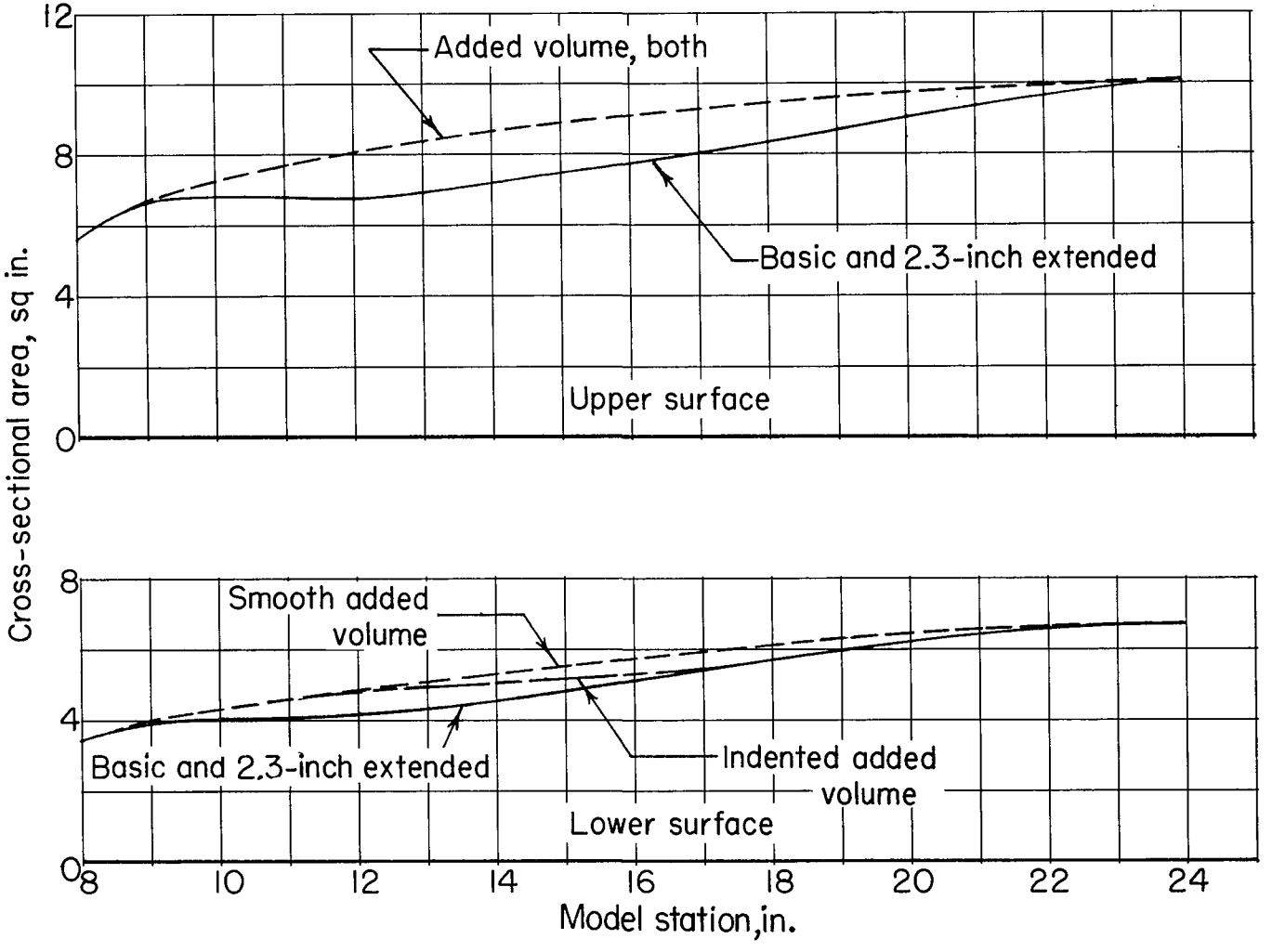


(b) Upper- and lower-surface distributions for the added-volume configurations.

Figure 3.- Continued.

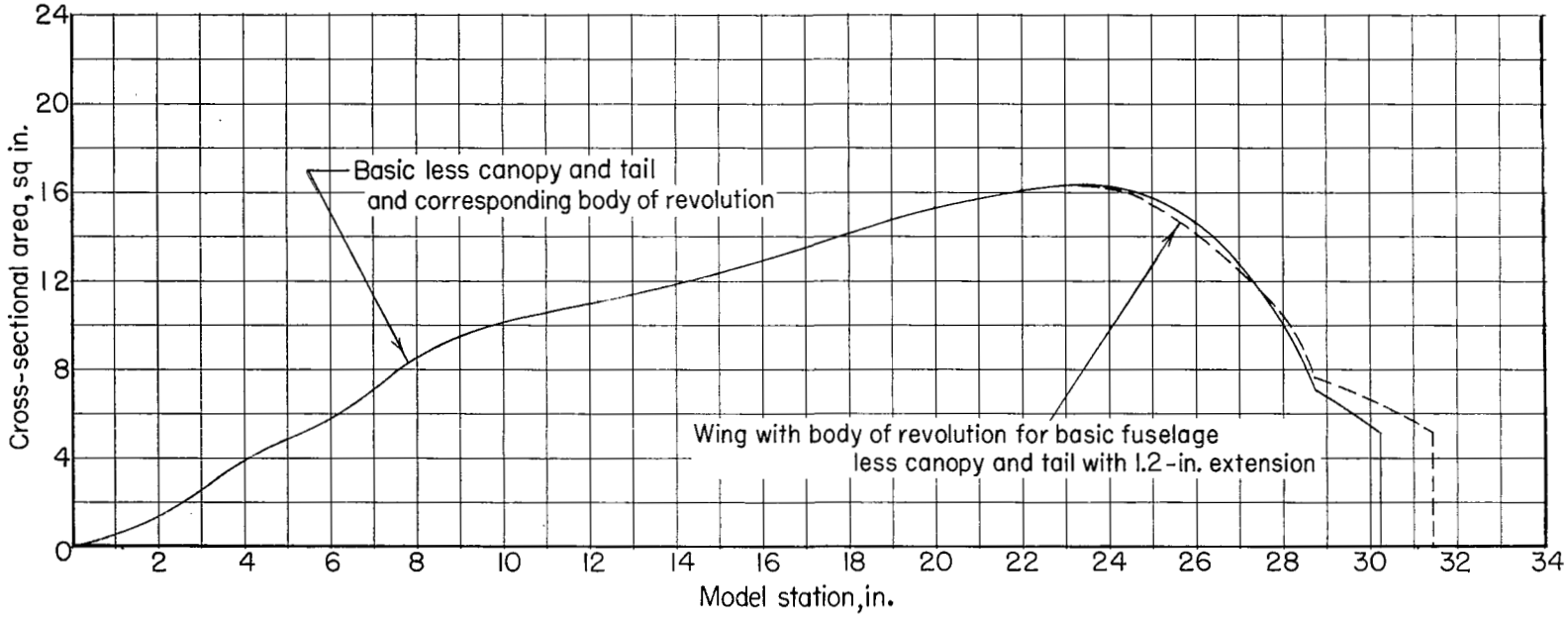


(c) Basic less canopy and tail, and wing with 1.2-inch-extended body of revolution for the basic fuselage less canopy and tail.

Figure 3.- Concluded.

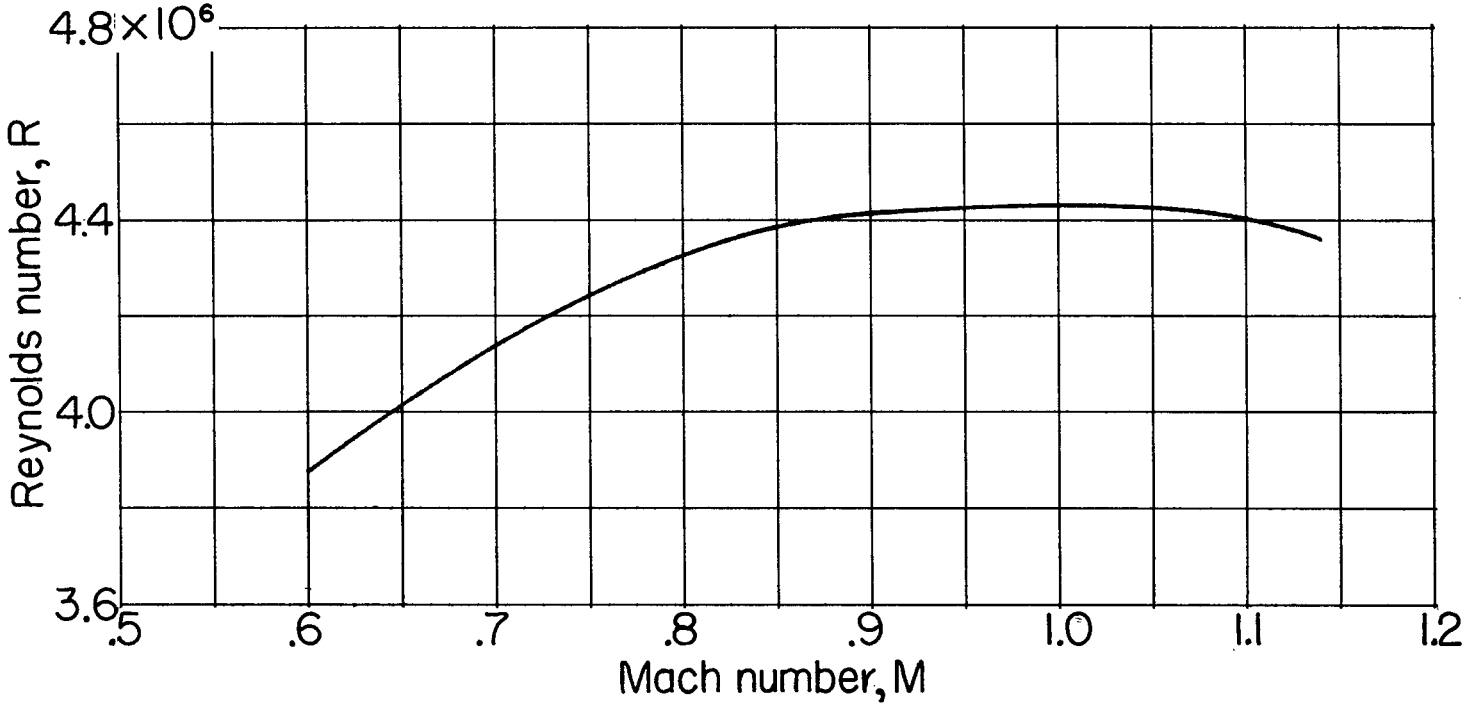


Figure 4.- Variation with Mach number of average test Reynolds number based on $\bar{c}$ = 13.755 inches.

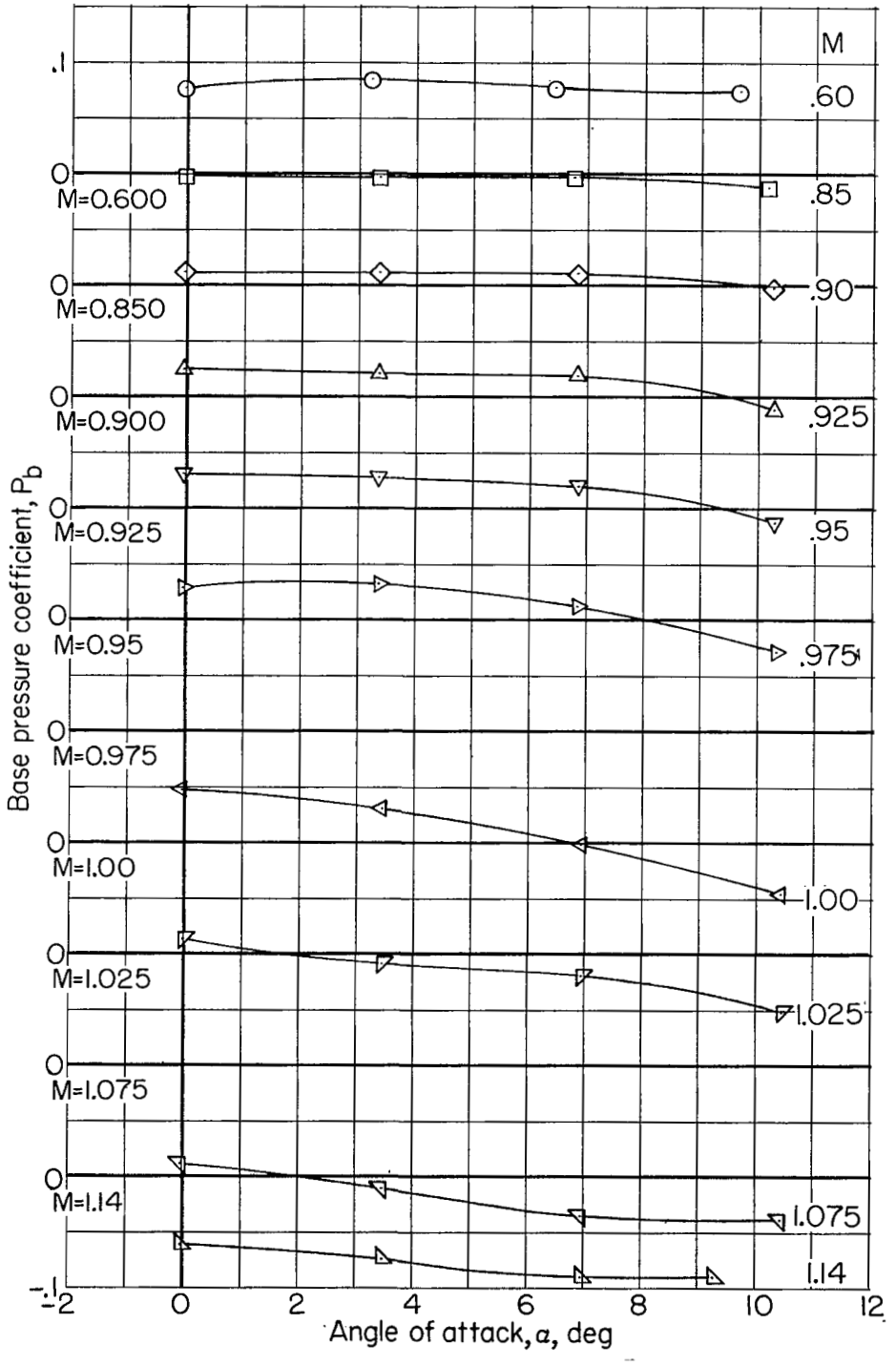


(a) Basic.

Figure 5.- Base pressure coefficients for the various configurations tested with the ducts closed.

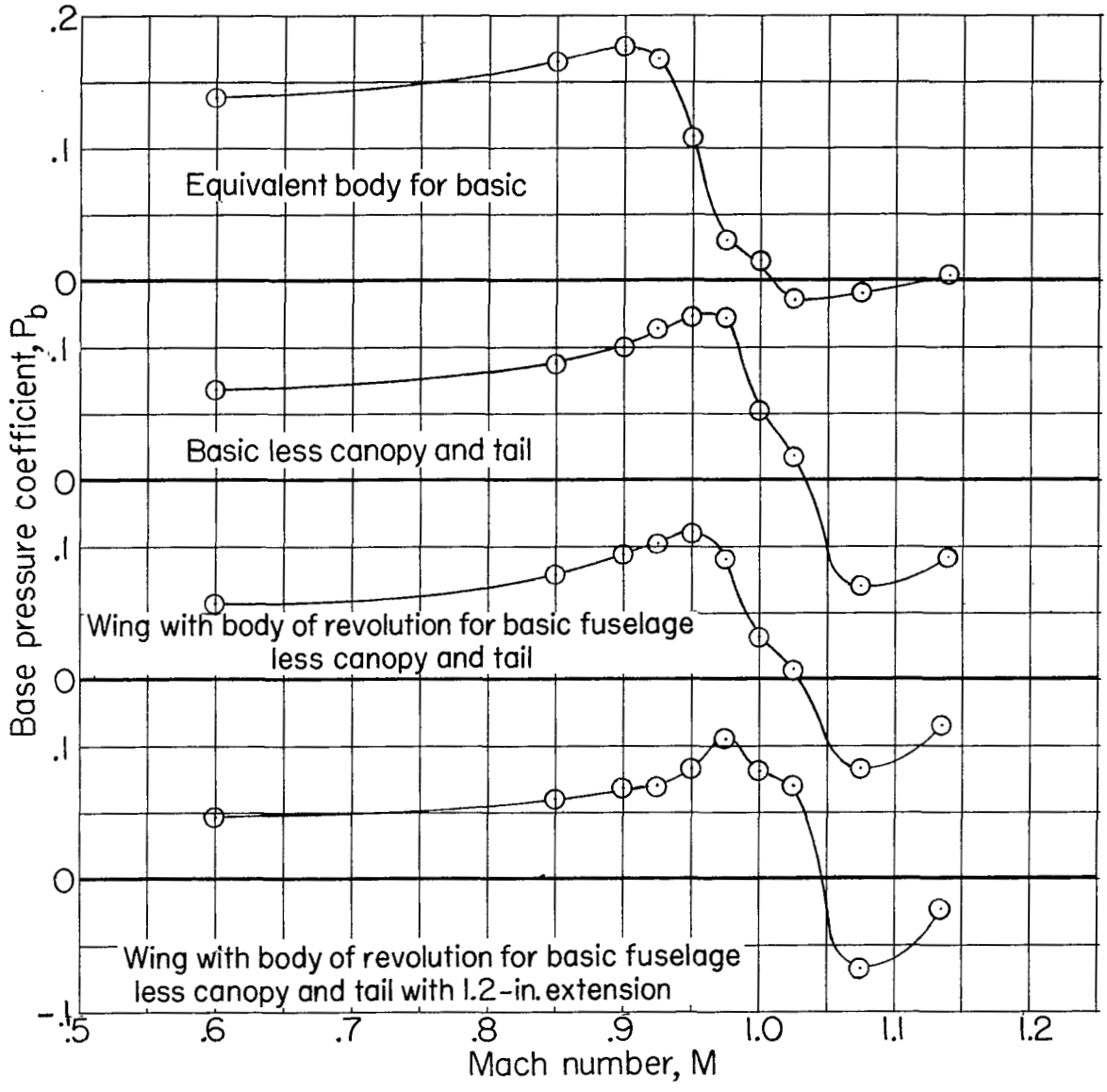


(b) Basic less canopy and tail, equivalent body, and wing with bodies of revolution. $C_L = 0$.

Figure 5.- Concluded.

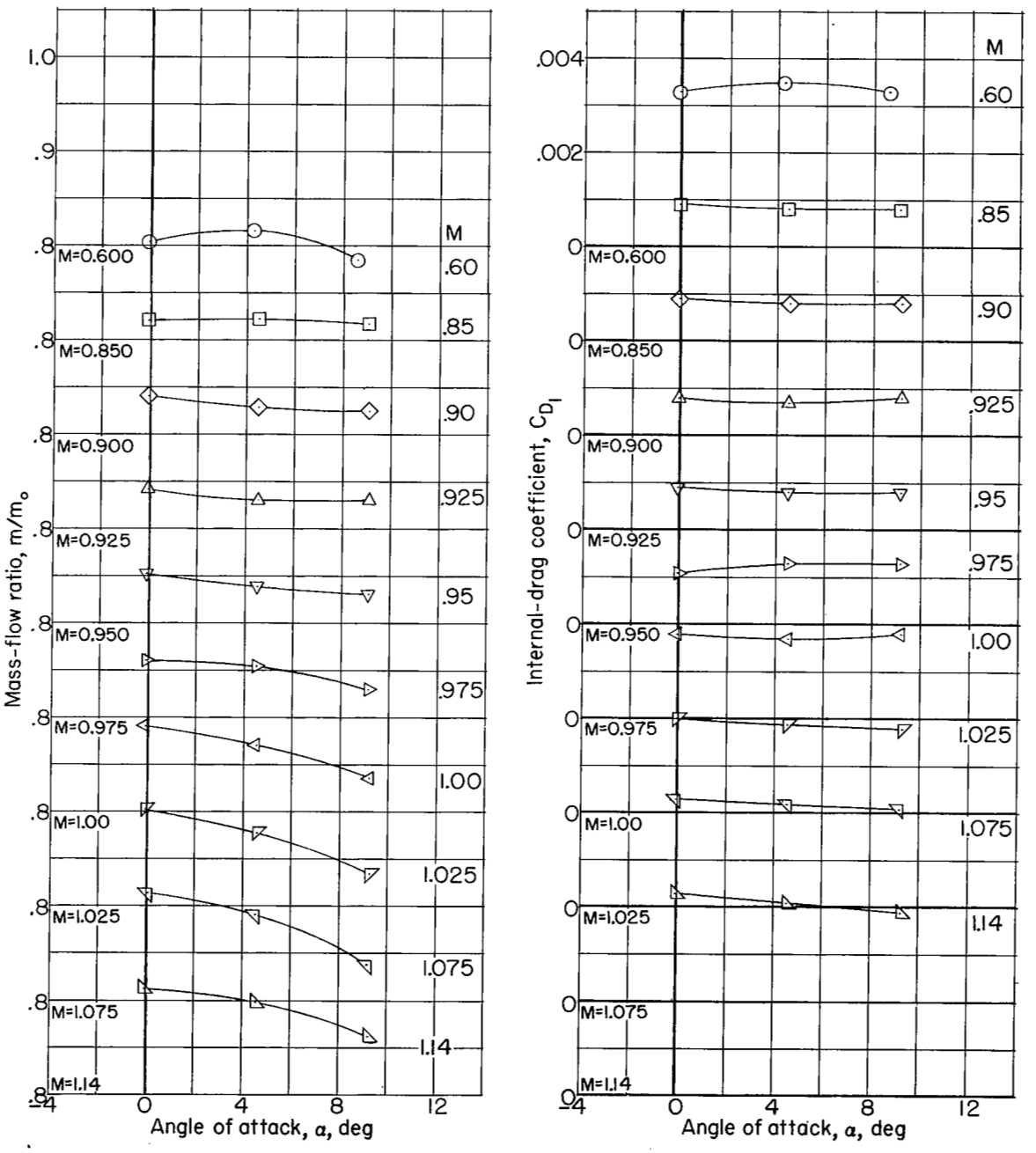


Figure 6.- Mass-flow ratios and internal-drag coefficients for the basic configuration. Ducts open.

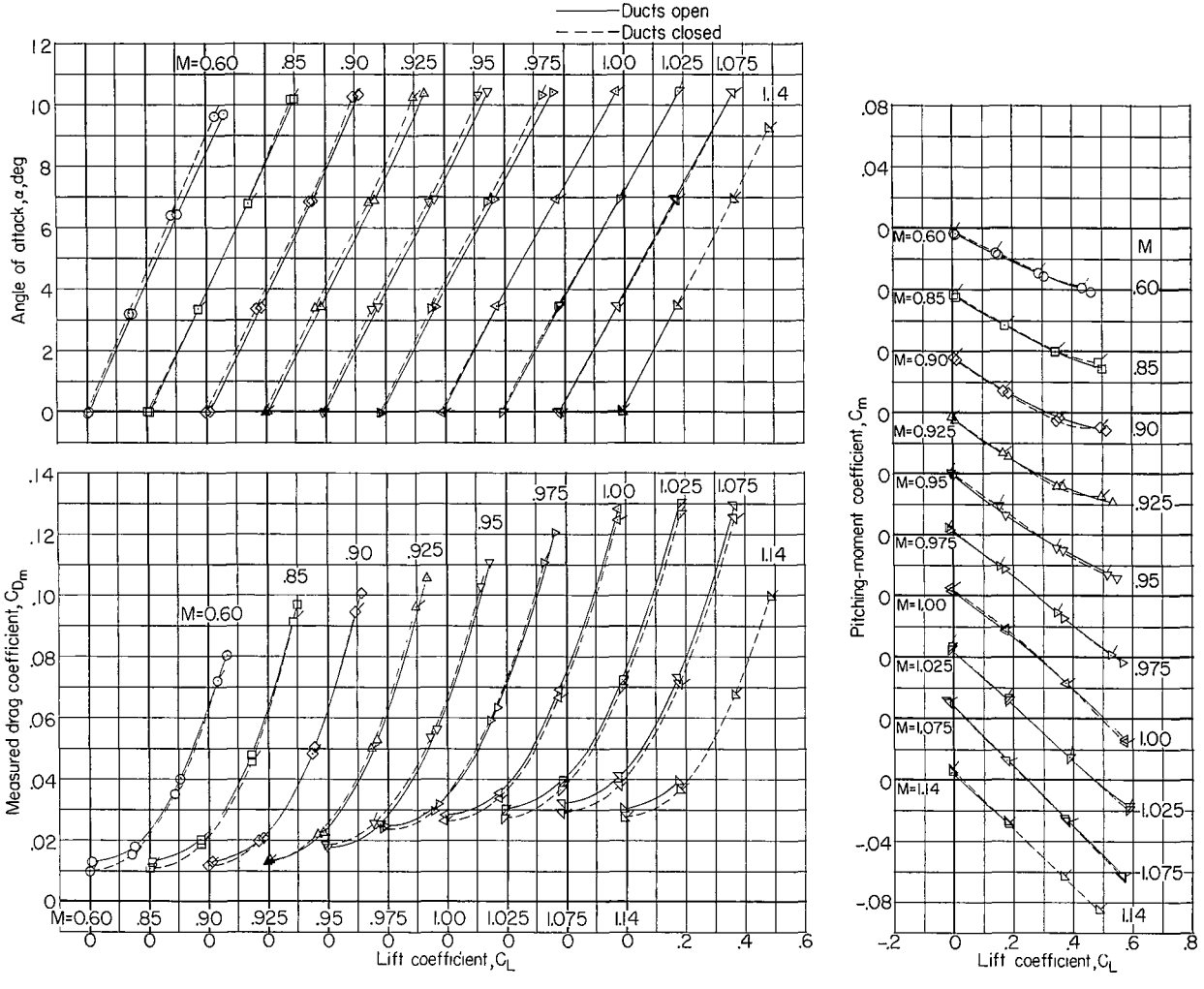


Figure 7.- Force and moment characteristics for the basic configuration with the ducts open and closed. Ducts-open data include internal drag.

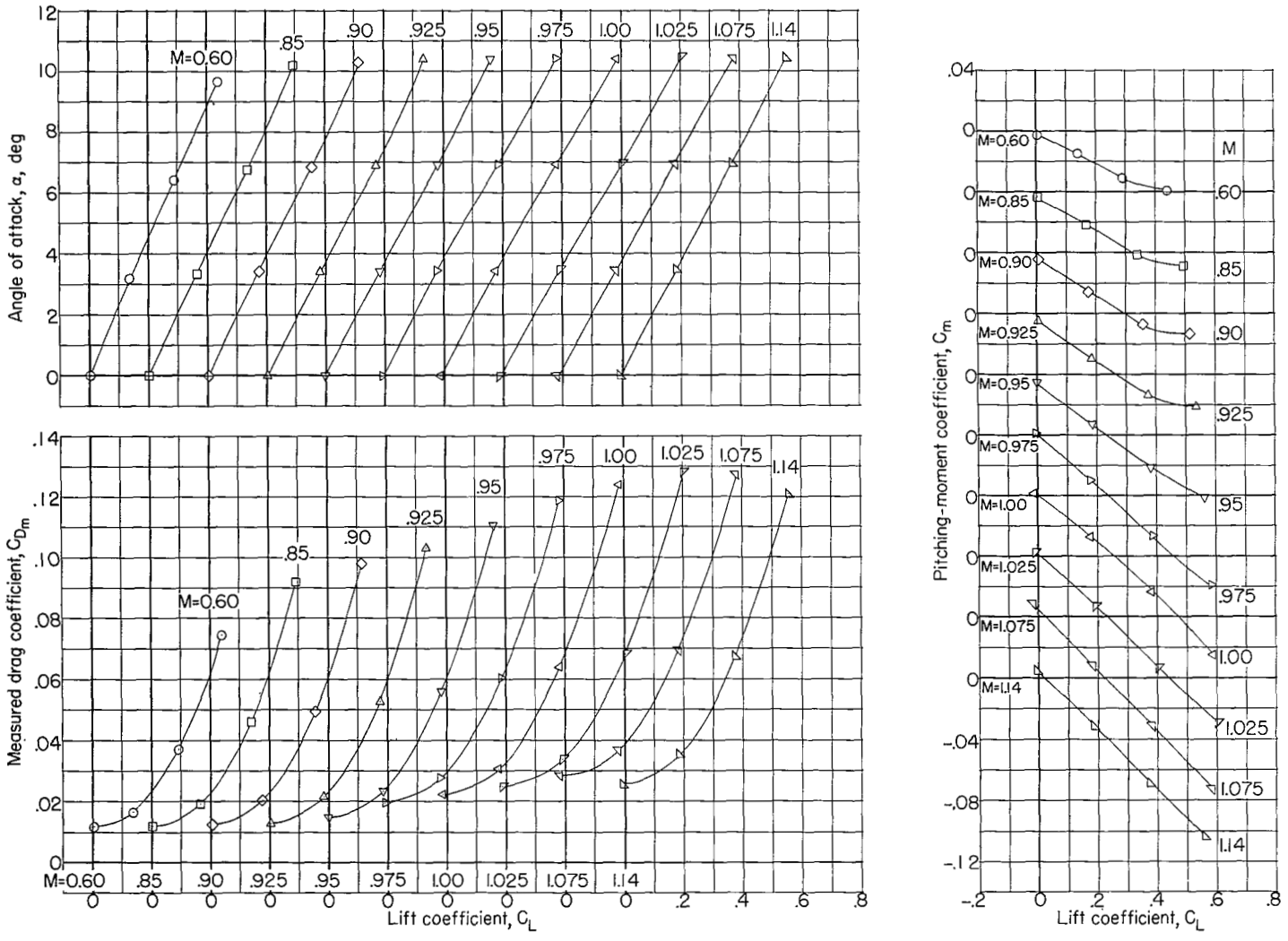


Figure 8.- Force and moment characteristics for the 2.3-inch-extended configuration with the ducts open. Data include internal drag.

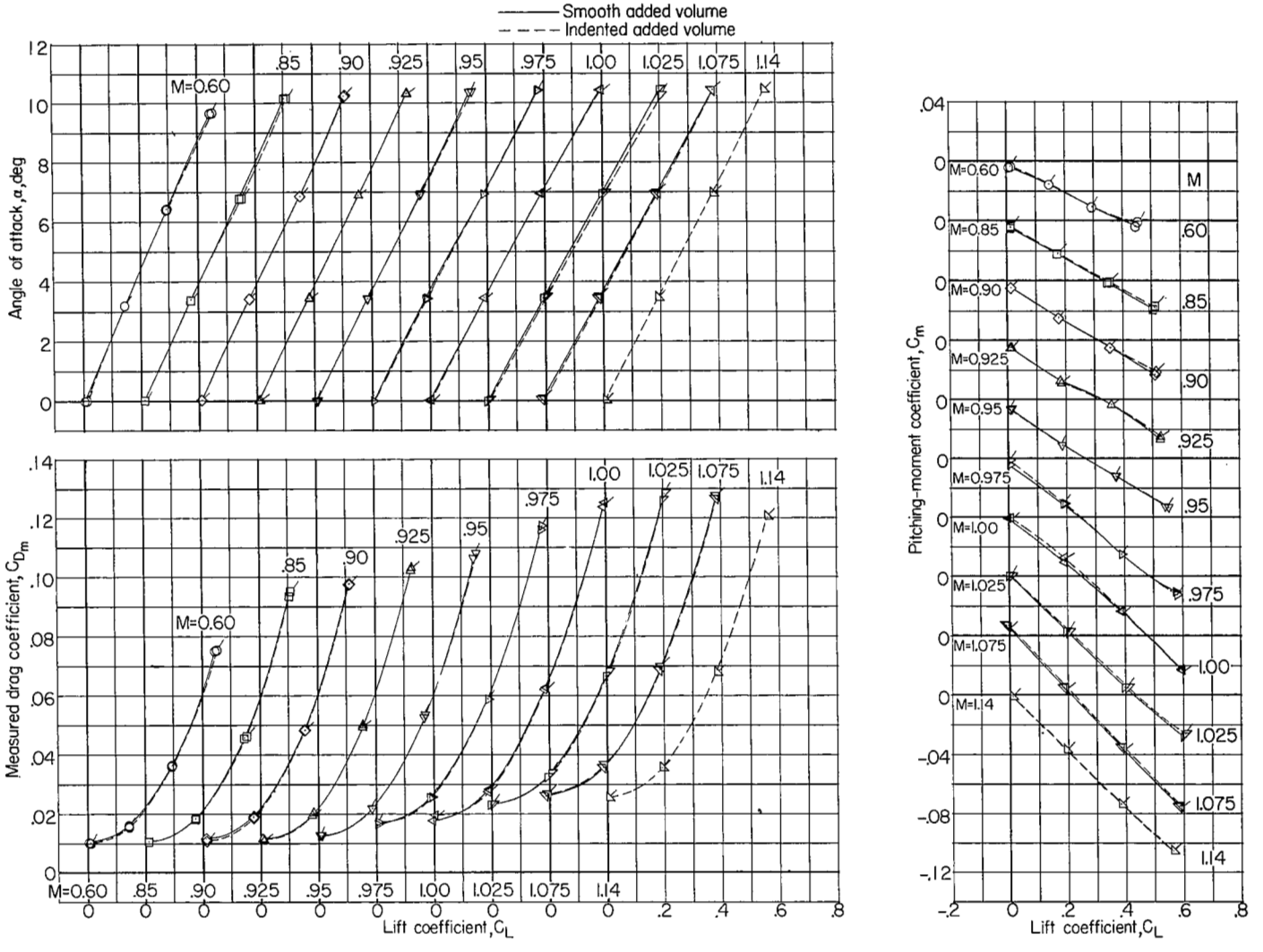


Figure 9.- Force and moment characteristics for the added-volume configurations with the ducts open. Data include internal drag.

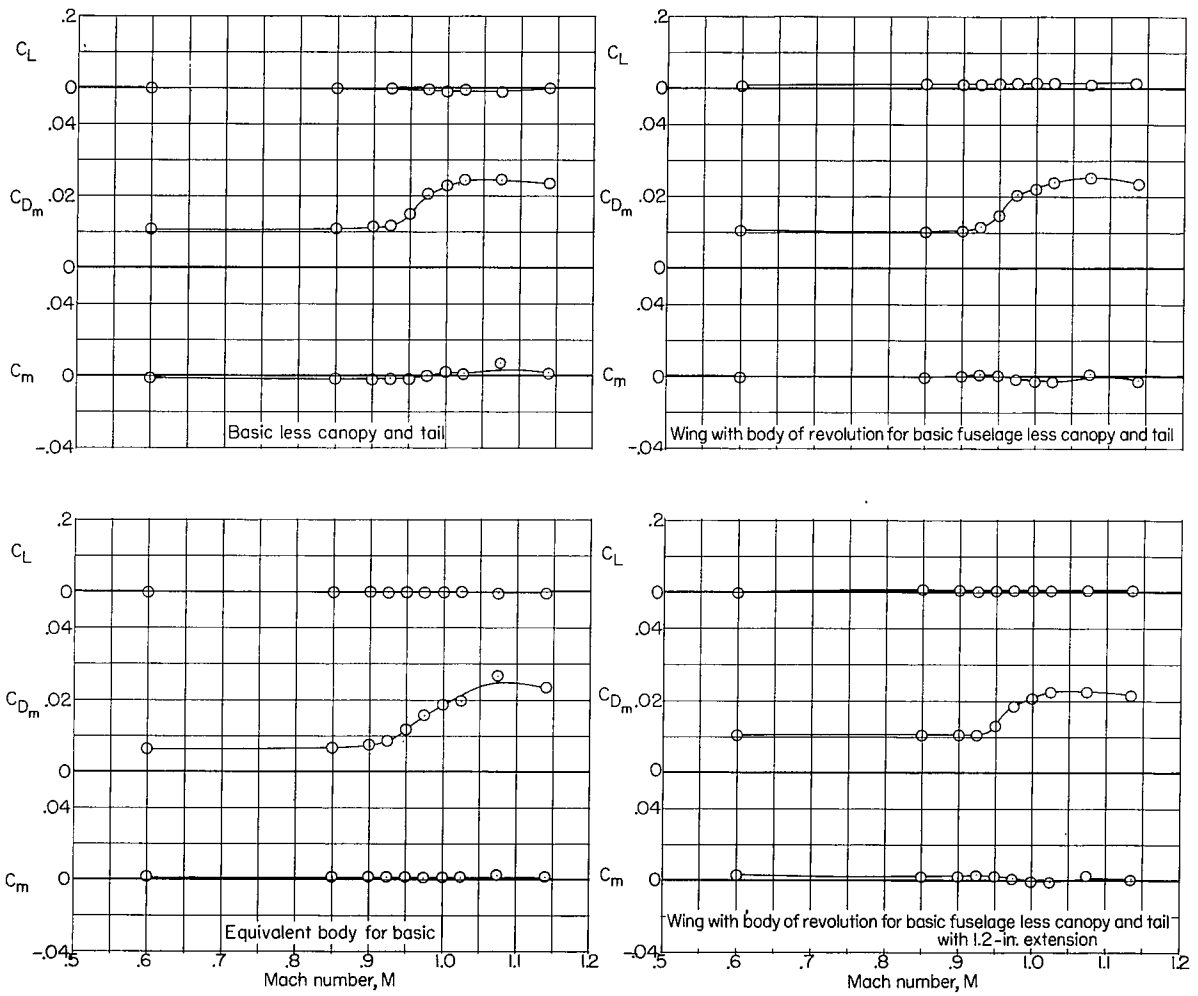


Figure 10.- Force and moment characteristics for the basic configuration less canopy and tail, the basic equivalent-body configuration, and the wing with the bodies of revolution. Ducts closed.

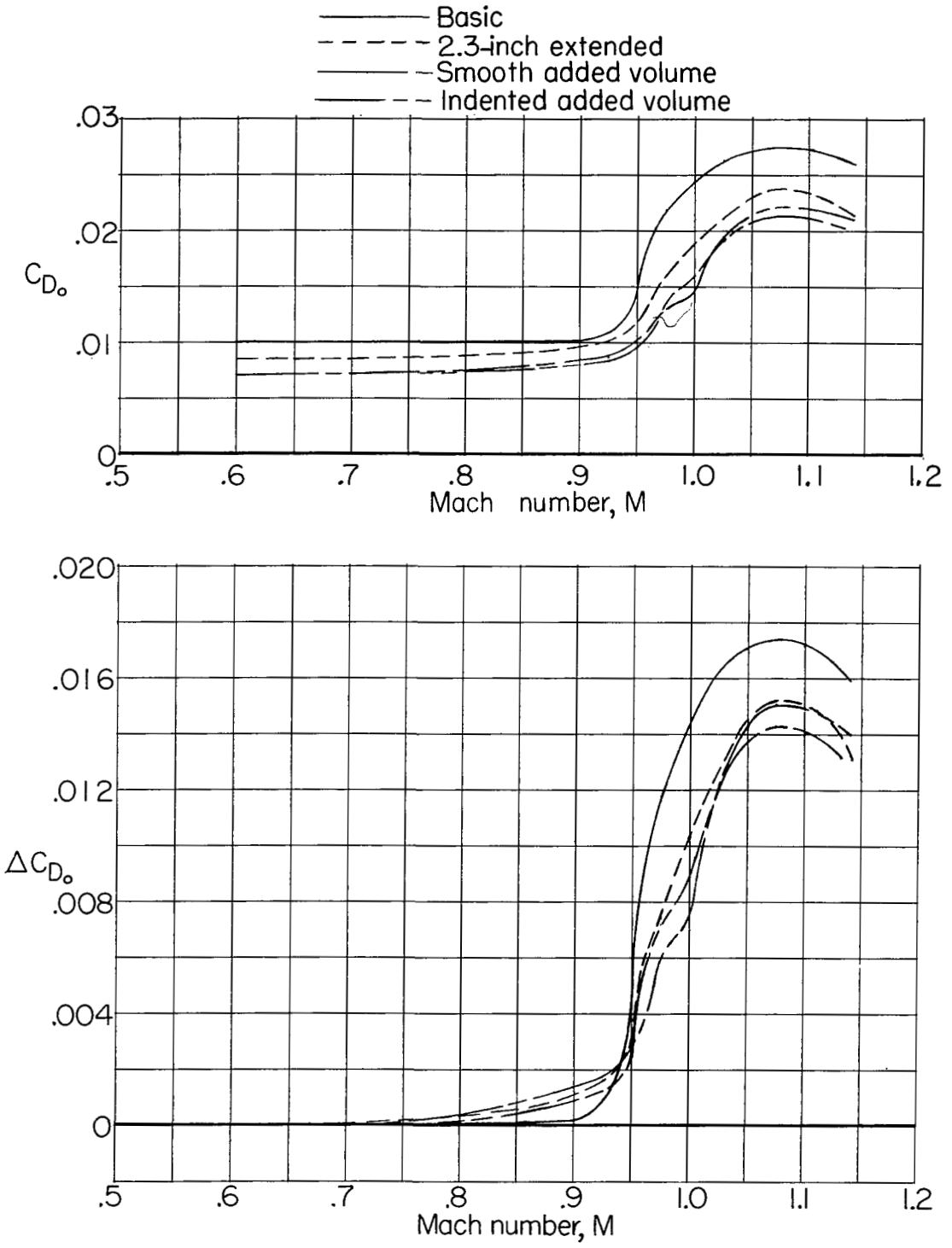


Figure 11.- Zero-lift and incremental zero-lift drag coefficients for the basic and modified fuselage configurations with the ducts open. Internal drag removed.

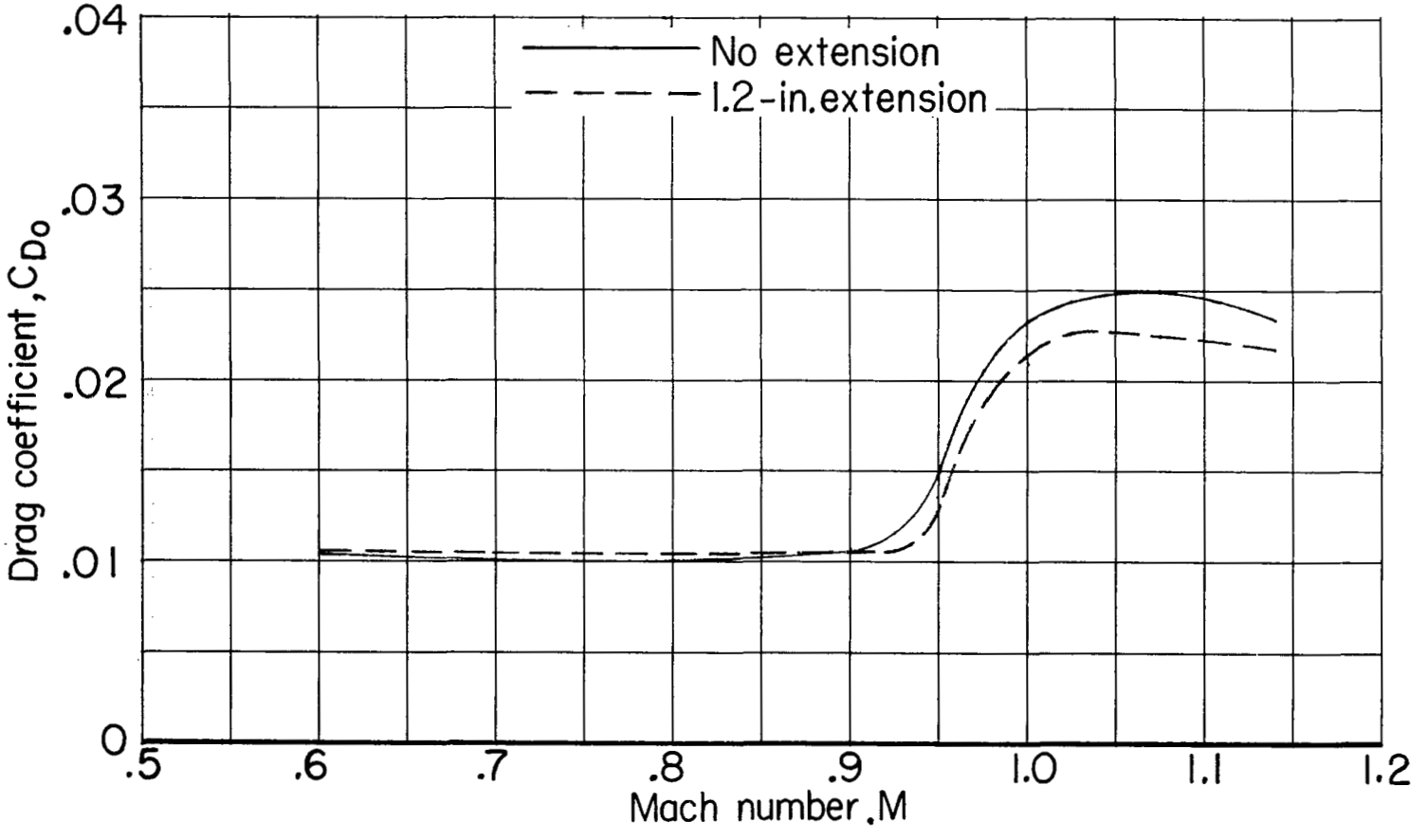


Figure 12.- Zero-lift drag characteristics for the wing with a body of revolution for the basic fuselage less canopy and tail and the wing with a 1.2-inch-extended body of revolution. Ducts closed.

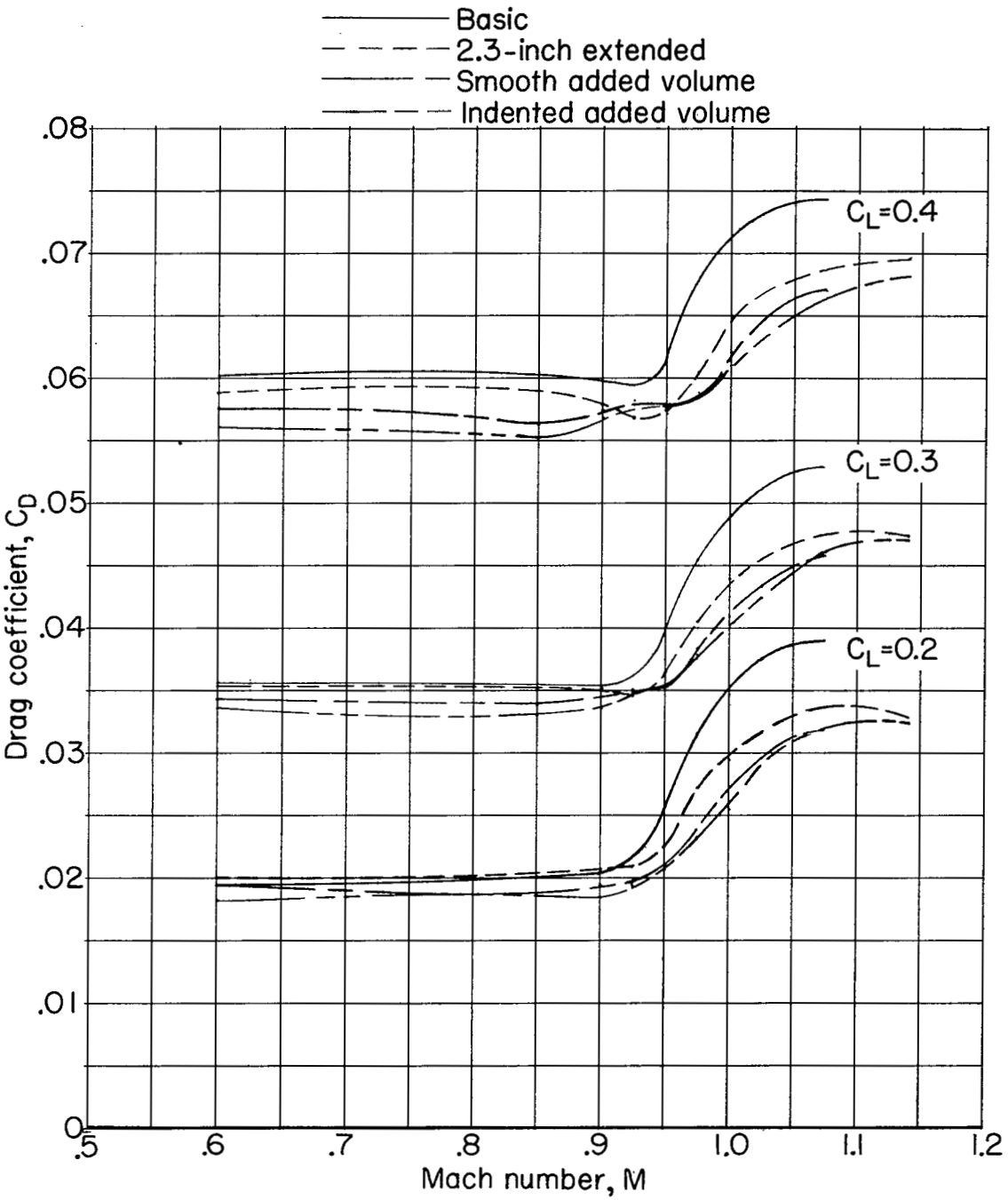


(a) Drag coefficient.

Figure 13.- Drag characteristics at lifting conditions for the basic and modified fuselage configurations with the ducts open. Internal drag removed.

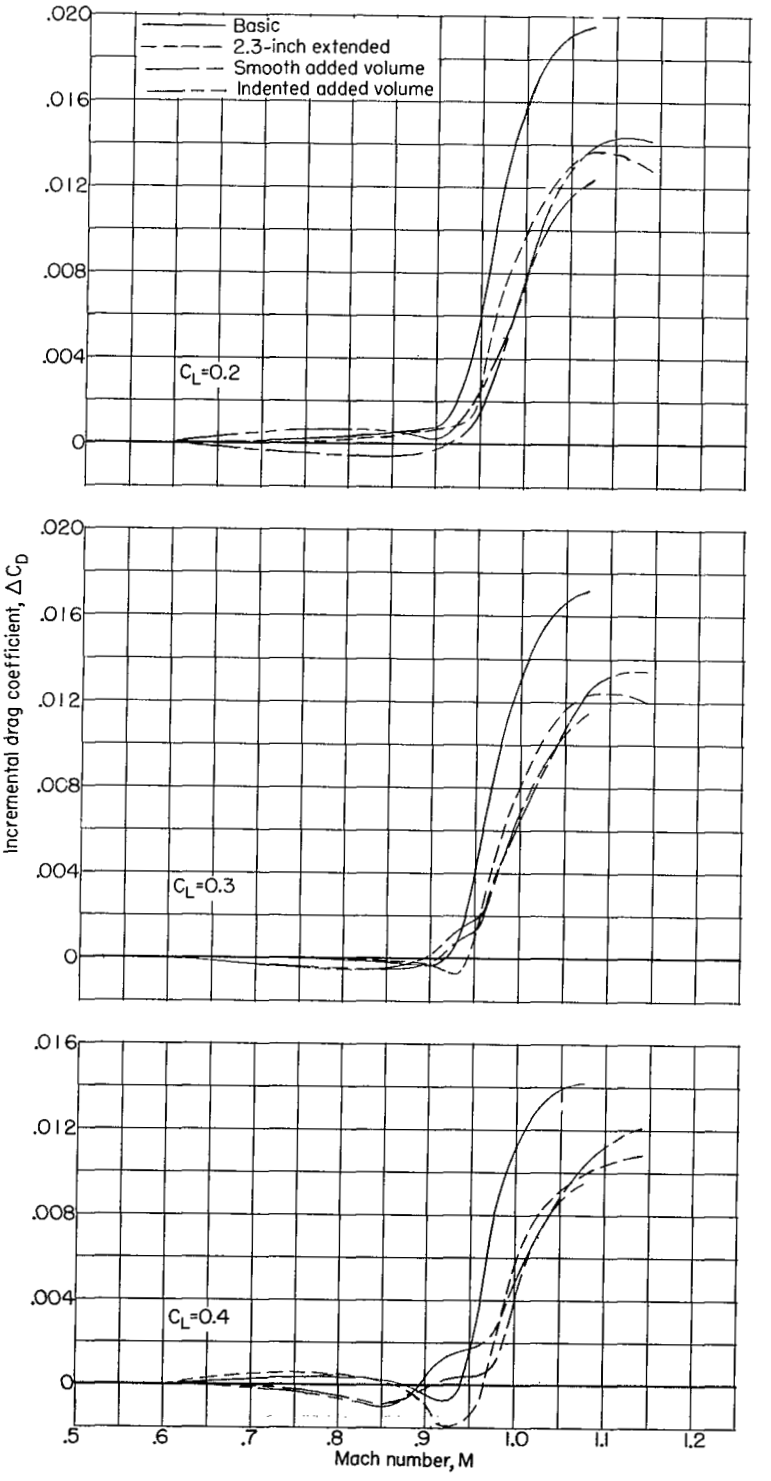


(b) Incremental drag coefficient.

Figure 13.- Concluded.

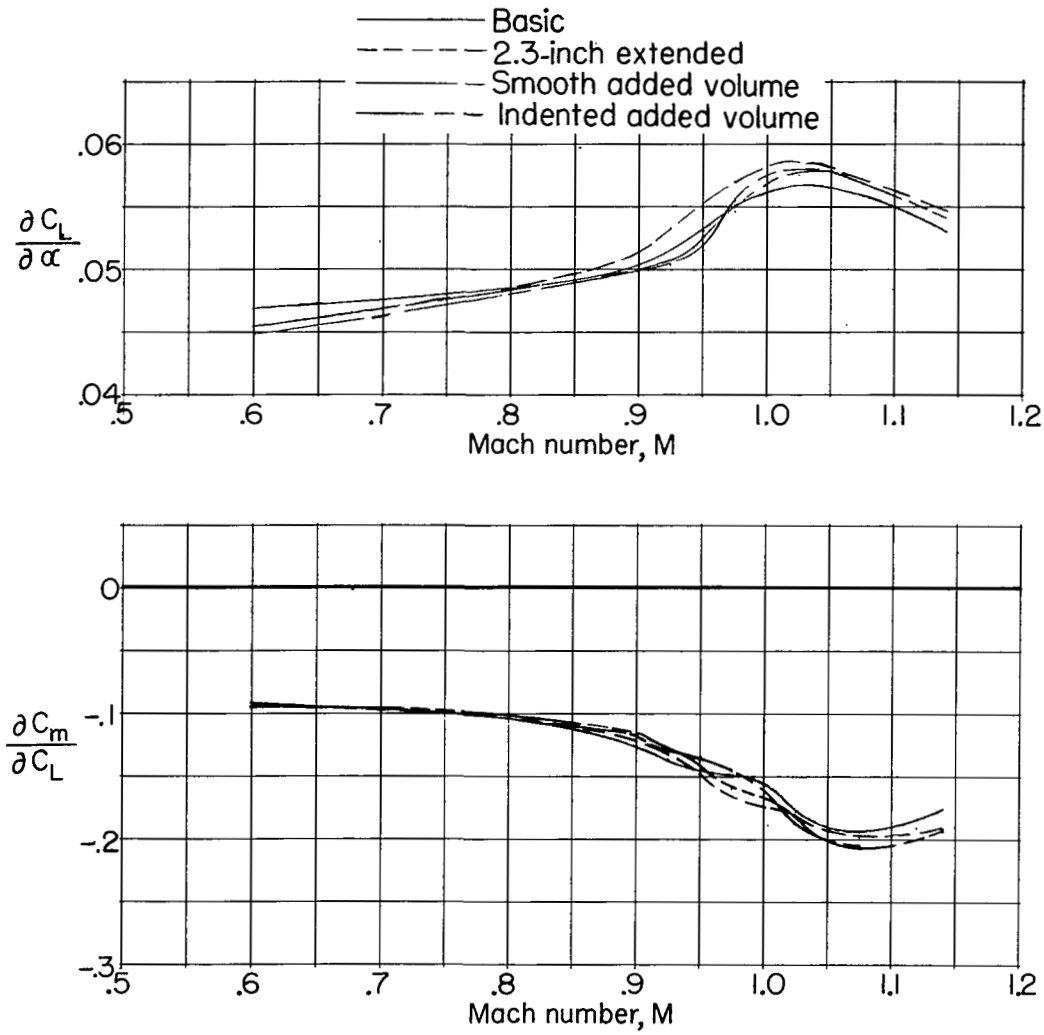


Figure 14.- Variation with Mach number of average lift-curve slopes and moment-curve slopes for the basic and modified fuselage configurations with the ducts open.

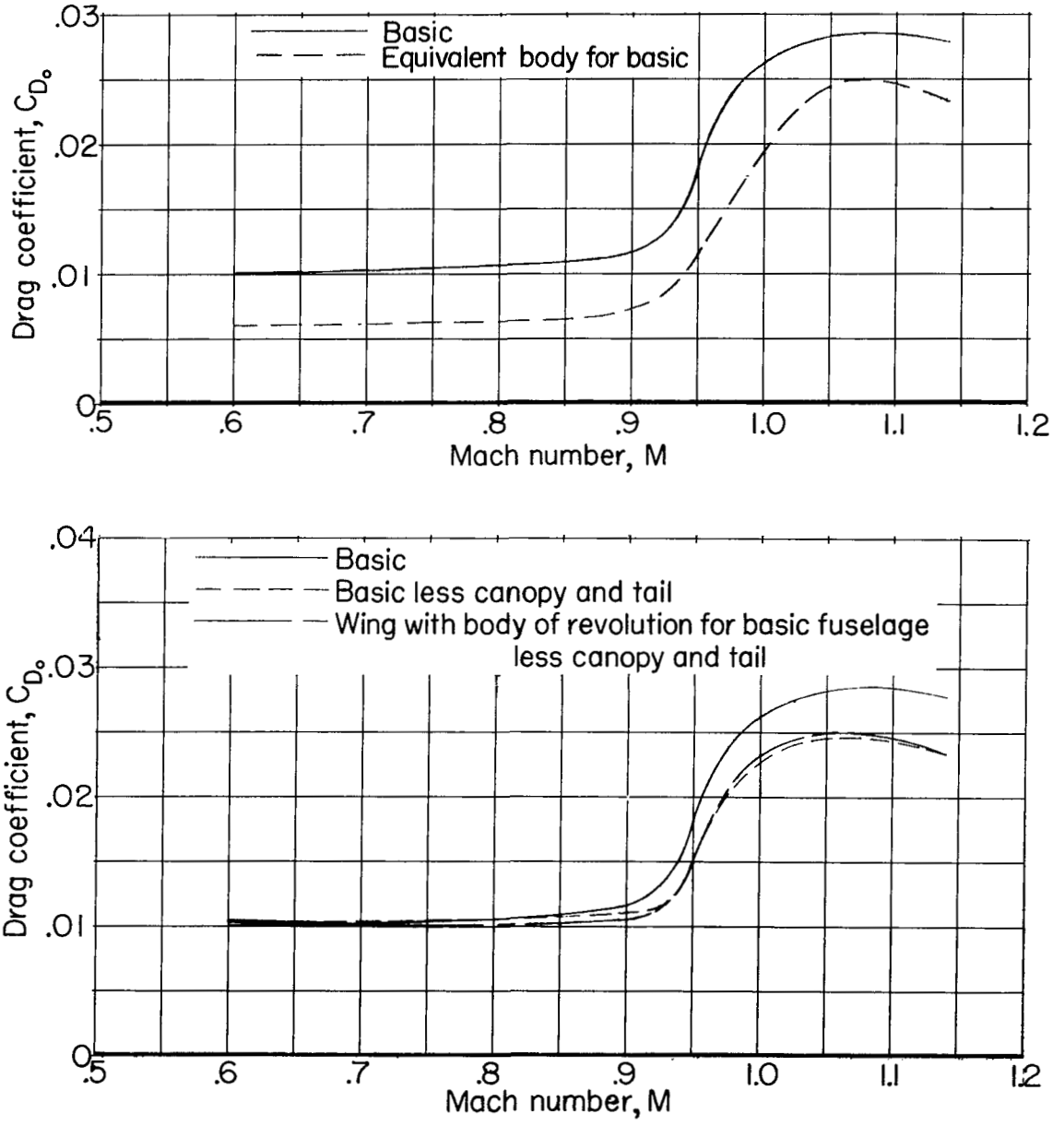


Figure 15.- Variation with Mach number of zero-lift drag coefficients for the basic configuration and its equivalent body, the basic configuration less canopy and tail, and the wing with a body of revolution for the basic fuselage less canopy and tail. Ducts closed.